



COPY RIGHT



ELSEVIER
SSRN

2023 IJEMR. Personal use of this material is permitted. Permission from IJEMR must be obtained for all other uses, in any current or future media, including reprinting/republishing this material for advertising or promotional purposes, creating new collective works, for resale or redistribution to servers or lists, or reuse of any copyrighted component of this work in other works. No Reprint should be done to this paper, all copy right is authenticated to Paper Authors

IJEMR Transactions, online available on 13th Apr 2023. Link

[:http://www.ijiemr.org/downloads.php?vol=Volume-12&issue=Issue 04](http://www.ijiemr.org/downloads.php?vol=Volume-12&issue=Issue 04)

10.48047/IJEMR/V12/ISSUE 04/136

Title **Battery Performance Analysis of Grid Integrated Electrical Vehicle in Different Modes of Operations**

Volume 12, ISSUE 04, Pages: 1063-1070

Paper Authors

Dr. P. Lakshman Naik, Sk. Chandini, Sk. Sameena, V. Pavani, S. Lakshmi Sowjanya



USE THIS BARCODE TO ACCESS YOUR ONLINE PAPER

To Secure Your Paper As Per **UGC Guidelines** We Are Providing A Electronic Bar Code

Battery Performance Analysis of Grid Integrated Electrical Vehicle in Different Modes of Operations

Dr. P. Lakshman Naik, Associate Professor Department of EEE,
Vasireddy Venkatadri Institute of Technology, Nambur, Guntur Dt., Andhra Pradesh.

Sk. Chandini, Sk. Sameena, V. Pavani, S. Lakshmi Sowjanya.
UG Students, Department of EEE,
Vasireddy Venkatadri Institute of Technology, Nambur, Guntur Dt., Andhra Pradesh.
lakshman.help1@gmail.com
skchandini1938@gamil.com, shaiksameena192@gmail.com,
pavanivallapuri2002@gamil.com, lakshmisowjanya1809@gmail.com

Abstract

The system proposed in this paper is for use with electric cars, integrated converter that allows battery charging from both along with a solar photovoltaic system and the power grid. The benefit of this system is that both sources use the same converter, reducing the quantity required components. A further approach is the inductor voltage detection. Removing the need for a current sensor to regulate power factor. All EV operating modes, including charging, propulsion, and regenerative braking, are supported by the suggested system. The system performs as an isolated secondary ended primary inductance converter when powered by the grid or solar PV. In the corresponding PRN and RBG modes, it performs as a boost converter and buck converter. The paper goes into detail about the components' designs for each mode. Based on the proposed configuration, the authors present results from simulations and experimental studies on a 1 kW set-up. The results demonstrate the suggested systems techno-economic competence in comparison to other topologies. In summary, the proposed system in this paper is an integrated converter for EVs. This converter may be used to charge from both the power grid and a solar PV installation. All EV modes are supported by the system, which also has an IVD approach for power factor adjustment. Results from simulations and experiments show the advantages of the suggested system.

Keywords: Electric vehicles, a solar PV system and inductor voltage detection.

1. Introduction

Owing to the depletion of fossil fuels and the environmental problems brought on by carbon emissions from transportation, many experts throughout the world are prioritising the study of electric cars. Lowering the price, charger size, and

charging time are only a few of the significant problems in this field. The storage system and charging infrastructure are two of the primary arguments for why electric vehicles are so expensive. EV charging systems are often constructed with semiconductor-based

power electronic converters and sensor components together with voltage and current sensors, passive components, etc. These components are typically expensive, which adds to the overall cost of EVs.

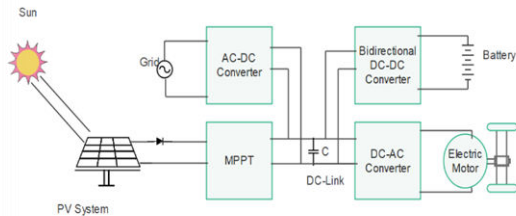


Fig.1. Block Diagram

Operational Modes.

We employed all three modes. The three operating modes include propulsion, plug-in charge, solar PV charging, and regenerative braking.

A. Charging Mode (Pin)

By providing a voltage signal to the switch " Sa_1 " the converter functions as an isolated SEPIC. Switches P_1 and P_3 are turned off, while switch P_1 is switched on. At activation of the semiconductor switch by the pulse width modulation signal Sa_1 , inductor L_1 and magnetizing inductor L_m . The capacitor C_b provides energy to the load during this process (battery). When switch Sa_1 is Inductors should be off. L_1 , L_m provide giving the capacitor energy C_s and the output. The DC-DC converter can provide power to the load (battery) even

when solar power is not available. SEPIC mode that is isolated.

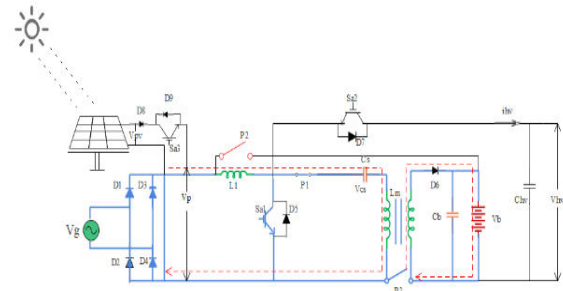


Fig2: Charging Mode (Pin)

B. Photovoltaic (PV) Mode

The system operates in two modes: when the solar power is below a certain threshold and when it is above that threshold. When solar power exceeds the threshold, a specific switch configuration is used, and the converter performs maximum power point tracking to charge the battery with the most available power. During such situations, the switch Sa_3 plays a role in enhancing the effectiveness of the PV panel, though it is unclear how it does so without more context.

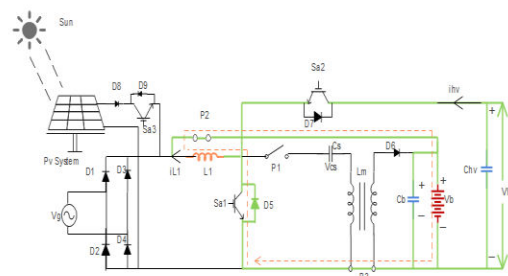


Fig 3: Photovoltaic (PV) Mode

C. PRN Mode

It seems that you are describing a specific circuit configuration where a

battery is being discharged to supply energy to a capacitor through a DC connection. The circuit includes switches P_2 and P_3 that are in an ON state, and an inductor L_1 that charges upon switching Sa_1 is used to ON. The direction of the current L_1 is shown by a solid line in the circuit diagram. When switch Sa_1 is turned OFF, the stored energy in the inductor L_1 is then supplied to the DC-link capacitor C_{hv} . The path of the current is shown with dotted lines in the circuit diagram. This process of charging and discharging the inductor L_1 can be used to regulate the voltage across the DC-link capacitor C_{hv} . and make certain that it remains stable. This kind of circuit This type of circuit is frequently used in power electronics applications like DC-DC converters and motor drives.

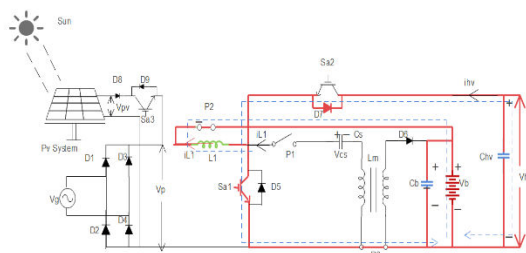


Fig4: PRN Mode

D.RBG Mode

You appear to be describing a mode of operation for an electric vehicle (EV) or hybrid electric vehicle (HEV) in which the

battery is charged via the motor drive system's regeneration process. Many modern EVs and HEVs have this feature. In this mode of operation, the battery is fed with the energy stored in the DC-link, extending the vehicle's range. To accomplish this, the SPST switches P_2 and P_3 are activated, and switch Sa_2 is activated to charge inductor L_1 via the DC-link source. Upon switching off switch "Sa2" the inductor L_1 discharges the battery by releasing its accumulated energy. Overall, this mode of operation contributes to the EV or HEV's efficiency and range by allowing it to recapture energy that would otherwise be lost during braking or deceleration.

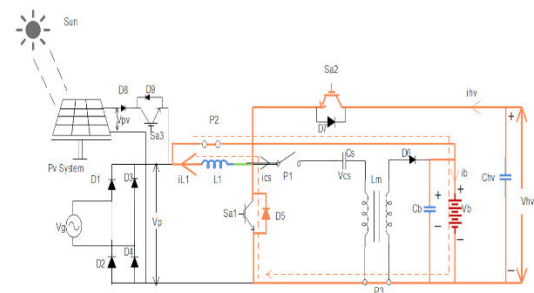


Fig 5: RBG Mode

2. Inductor and capacitive element calculations

A. Inductor L_1 PIN Charging Mode Design

The inductor is used in each mode, and the system's ultimate value is chosen from the biggest value obtained from each mode. The first described mode is PIN charging, in which the voltage across the inductor is given by

$$V_{L1} = |V_g| L_1 \frac{di_{L1}}{dt} = L_1 \frac{\Delta i_{L1, PIN}}{d1T_s}$$

It is denoted as the L_1 in PIN Mode

$$(L_{1,PIN}) \quad L_{1,PIN} = \frac{Vg^2}{P_g f_s X\%} \frac{V_b}{V_g + V_b}$$

Using the above equations, we obtain

$L_{1,PIN}$ 3.5Mh by the ripple of 30% of i_g .

Solar PV mode

The inductor value in the solar PV mode identifies as $L_{1,PV}$. The demonstration of $L_{1,PV}$ is

$$L_{1,PV} = \frac{V_{PV} d_2}{\Delta i_{L_{1,PV}} f_s}$$

$$D_2 = \frac{V_b}{V_{PV} + V_b}$$

$$L_{1,PV} = \frac{v^2 PV}{P_{PV} f_s \varepsilon\%} \frac{v_b}{v_{pv} + v_b}$$

We get the by solving those equations with a ripple factor of 30%. $L_{1,PV}$ is 3.63mH.

PRN MODE

The Sa_1 switch is on, the inductor's voltage is raised. L_1 , provided as follows :

$$V_b = L_1 \frac{di_{L_1}}{dt} = L_1 \frac{\Delta i_{L_1,PRN}}{d_3 T_s}$$

The value of inductor L_1 of the PRN Mode denoted as $L_{1,PRN}$. The equation is follows

$$L_{1,PRN} = \frac{d_3 V_b}{\Delta i_{L_1,PRN} f_s}$$

By using those above equations assume the $\eta = 30\%$, then the $L_{1,PRN}$ is 2.65 MH.

RBG Mode

When Sa_2 , switch is on the voltage across the inductor L_1 , in the below Equations :

$$v_{hv} - v_b = L_1 \frac{\Delta i_{L_1,RBG}}{d_4 T_s}$$

In the RBG Mode it can be denoted as the $L_{1,RBG}$

$$L_{1,RBG} = \frac{V_{hv} d_4 (1-d_4)}{\Delta i_{L_1,RBG} f_s}$$

Whenever the assume the μ value 30%, then the value of the $L_{1,RBG}$ is 2.63 MH. Comparing the above all mode values, we find that the maximum value is $L_1 = 3.63$ MH. Therefore, the final value of L_1 is 3.6MH.

B. Design of L_m (Magnetising inductance)

The PIN and Solar PV modes will calculate the magnetising inductance design.

PIN Charging Mode

The magnetising inductor's value is calculated $L_{m,PIN}$ for a PIN charging mode. The calculation begins with the voltage input. V_b , which is multiplied by $(1-d_1)$, where d_1 is the converter's duty cycle

$$L_{m,PIN} = V_b \frac{(1-d_1)}{\Delta i_{L_m,PIN} f_s} = \frac{Vg^2}{P_g} \frac{1}{\pi\% f_s} \frac{V_b}{V_g + V_b}$$

Finally, the text specifies the value of for. $L_{m,PIN}$ The allowed a 30% ripple at the moment is calculated to be 3.5 MH.

PHOTO VOLTAIC (PV) Mode

L_m is a parameter related to the inductor used in a DC-DC converter, and its design expression is L_m . In the PV (photovoltaic) mode, the expression for L_m is indistinguishable from the PIN charging mode, which is given by:

$$L_m = V_b \frac{(1-d_2)}{\Delta i_{L_m,PV} f_s} = \frac{V_{pv}^2}{P_{pv}} \frac{1}{\gamma\% f_s} \frac{V_b}{V_{mp} + V_b}$$

L_m value is computed as 3.23 MH for a 30% allowed ripple in the current. Finally, the maximum L_m (PIN) and L_m are chosen L_m (PV). The value of L_m (PIN) is not specified in the excerpt.

C. Design of Capacitor Cs

With the given values of V_g , \max , k , f_s , and p_b , the capacitance value can be calculated. After determining C_s , the voltage ripple across C_s can be calculated as:

$$C_s = \frac{V_b d_1(t)}{KV_{cs}(t)f_s R_L}$$

$$C_s = \frac{V_b}{k|V_g(t)|f_s \frac{V_b^2}{P_b}} \left(\frac{V_b}{|V_g| + V_b} \right) = \frac{P_b}{k f_s (|V_g| + V_b)}$$

We can calculate C_s by solving the above equations. As a result, we chose 1F.

D. Design of Capacitor C_b and C_{hv}

The following is the equation for determining the capacitance value of capacitor C_b

$$C_b = \frac{I_b}{2\omega\Delta V_{cb}} = \frac{\frac{P_h}{V_b}}{2\omega\delta\%V_b} = \frac{P_b}{2\omega\%V_b^2}$$

Using those equations, we can calculate the capacitance C_b to be 1200F for a ripple factor of 5% voltage.

The DC-link Capacitor's equation.

$$C_{hv} = \frac{d_3}{Rf_s \frac{\Delta V_{hv}}{V_{hv}}}$$

3. TECHNIQUE CONTROLLERS

Controller for solar PV charging and PIN charging:

the numerous grid-side power factor correction (PFC) regulation methods, with a focus on reducing the complexity of traditional techniques. Some authors have proposed fewer sensing circuits for PFC operation, such as the nonlinear carrier (NLC) control technique, which compares switch, diode, To achieve high power factor circumstances, inductor

current with carrier waveforms is used throughout each switching cycle. These techniques, however, still necessitate the use of a current sensing circuit. The following paragraph describes the approach for PFC in continuous conduction using inductor voltage detection (IVD) (CCM). This method involves sensing the inductor voltage with By adding a little winding to the same inductor core and rectifying the measured signal, only the positive component is left. This method is preferable for on-board charger (OBC) applications because it is straightforward, affordable, and comparable to voltage mode control approaches used in circuit implementation.

Across the inductor L_1 , the switching period voltage is

$$V_{L1} = V_g(d_1) + (V_g - V_{cs} - V_b)(1 - d_1)$$

The rectified voltage of the V_{L1}^* equation is

$$V_{L1}^* = V_g d_1 = \frac{1}{T_s} \int_0^{d_1 T_s} V_{L1}^*(T) d_T$$

This equation represents the voltage drop across the switch.

$$i_s R_s = R_g i_g d_1 = \frac{R_s}{L_1} \int_0^{d_1 T_s} V_{L1}^*(T) d_T$$

The average inductor voltage value is

$$V_q = \frac{R_s}{R_e T_s} \int_0^{d_1 T_s} V_{L1}^*(T) d_T$$

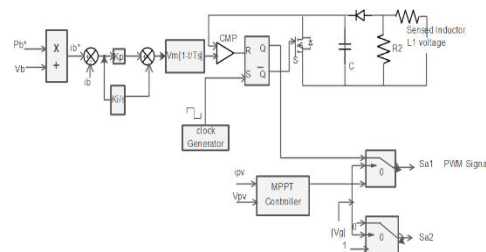


Fig 6: PIN Charging and RBG Modes Control Circuit

PRN Charging and RBG Modes Control Circuit

PRN mode's control objective is to keep the DC-link voltage constant for the effective operation of the driving system for the vehicle. Using a dual-loop proportional and integral (PI) controller technique, the PRN mode receiving the difference in error between the reference DC-link voltage and the measured DC-link voltage through the outer loop PI controller. The output of the outer PI controller is compared to the measured battery current error signal by the inner PI controller. When a high-frequency sawtooth carrier signal is compared to the output of the inner PI controller, PWM pulses for the switch are produced Sa_1 . For efficient operation, the RBG mode control logic also employs dual loops. The RBG mode's control logic employs torque or speed as reference components to exploit the energy generated by motor inertia. During the RBG operation, charge the battery. The output of the outer PI controller is a reference charging power that generates the reference battery current for the inner current controller. Both PRN and RBG modes share the same inner PI controller. The inner controller's output is versus the sawtooth carrier signal, PWM pulses are produced to switch Sa_2 .

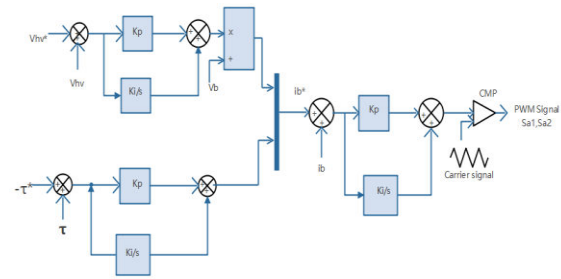
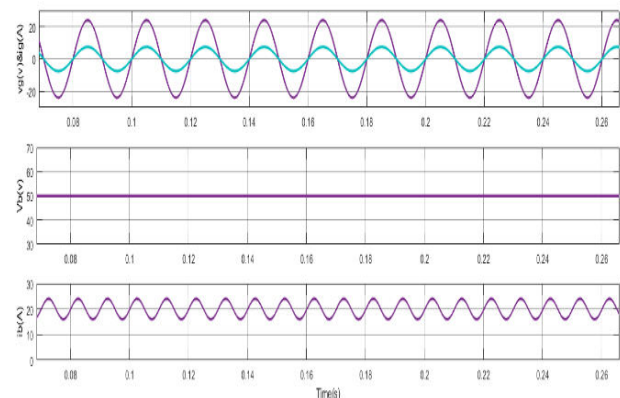


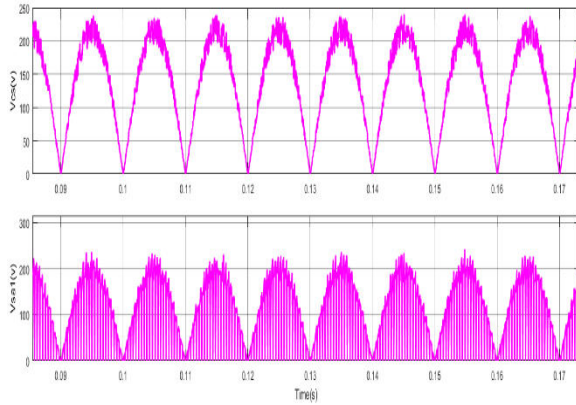
Fig 7: PRN Charging and RBG Modes Control Circuit

4. RESULTS OF SIMULATION

A. Charging Mode with a PIN

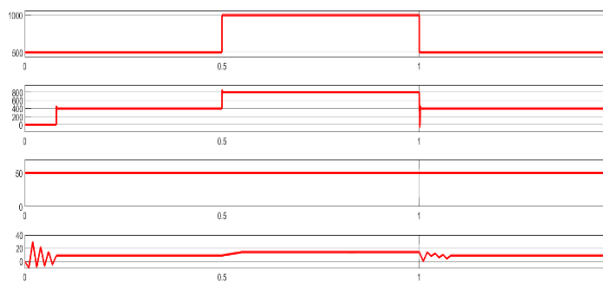
The depicts the relevant waveform for this mode. The grid voltage and current are perfectly sinusoidal because they are in phase. nature, as illustrated in Fig, demonstrates the success of the control approach. The (V_b) at 20% SOC, as well as the (i_b). With 1 kW charging power, the battery voltage is around 50V and the average battery current is 20 A. The voltage waveform applied to capacitor c_s . This capacitor's peak voltage is the same as the peak grid voltage he switch's voltage sa_1 the total of the grid and battery voltages ($v_g + v_b$), seen in the results.





B. Charging Mode with a Photovoltaic (PV)

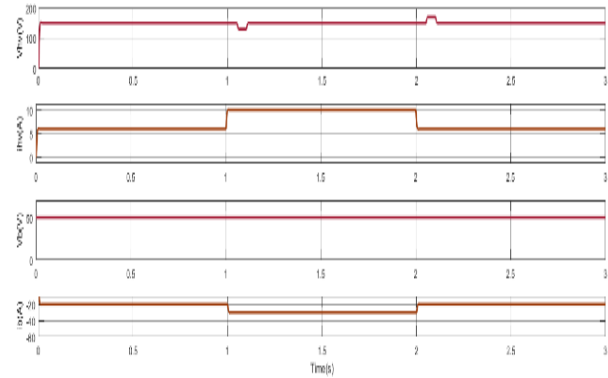
The suggested converter system's PV parameters. This mode's simulated waveforms. The MPPT operation is validated by varying the radiation from the sun in steps from 500 W/m² to 1000 W/m² and the greatest PV power in steps from 400 W to 800 W, respectively. The V_b and i_b waveforms are respectively. The V_b is nearly 50 V, the i_b ranges from 7.6 to 8.6.



C. Charging Mode with a PRN

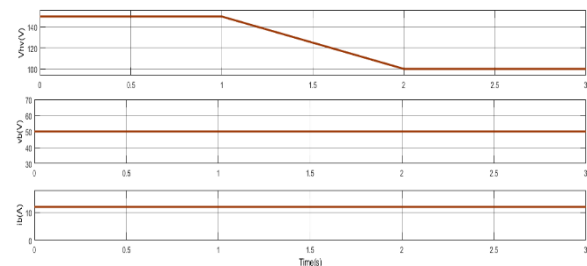
By charging the DC-link capacitor in this mode, the energy from PIN charging and RBG modes is utilised to power the vehicle's acceleration. This mode's control objective is to maintain the DC-link voltage. (V_{hv}) constant regardless of system variations. A step load variation of between 1 and 1.5 kW is used to test the viability of this mode. V_{hv} is regulated at a

reference value of 150 V, Figures show the V_b and i_b , respectively.



D. Charging Mode with a RBG

By charging the DC-link capacitor, the vehicle is propelled forward in this mode using the energy stored in the battery during PIN charging and RBG modes. This mode's control goal is to maintain a constant DC-link voltage (V_{hv}) regardless of system variations load is shown in Graphs.



5. Conclusion

The revolutionary on-board power integrated converter for electric cars that is suggested in this research has fewer components and is more suited for on-board applications. The suggested system uses the same portion of the converter to charge batteries from grid power and solar PV, respectively. The converter can be smaller since the system uses the inductor voltage detection method instead of a single sensor for power factor

adjustment. The results of both simulations and experiments are nearly identical, demonstrating the effectiveness of the proposed converter.

6.Future Scope

Electric vehicle that is powered by home electricity or solar energy. This means that electric vehicle owners will have to plan long trips and camping trips. A home-built electric vehicle will reduce the family's carbon footprint while also lowering electricity bills. Electric vehicles have enormous future potential. The charging station is the obvious starting point for these vehicles. However, this is only the first step in a potentially long journey that will include charging banks and other industrial areas, as well as homes and cities.

References

- [1].A. K. Singh and M. K. Pathak, "A multi-functional single-stage power electronic interface for plug-in electric vehicles application," *Electric Power Components and Systems*, vol. 46, no. 2, pp. 135–148, 2018.
- [2]. V. D and V. John, "Dynamic modelling and analysis of buck converter based solar PV charge controller for improved MPPT performance," in *2018 IEEE International Conference on Power Electronics, Drives and Energy Systems (PEDES)*, pp. 1–6, Dec. 2018.
- [3]. S. A. Singh, G. Carli, N. A. Azeez, and S. S. Williamson, "Modelling, design, control, and implementation of a modified z-source integrated PV/grid/EV dc charger/inverter," *IEEE Transactions on*

Industrial Electronics, vol. 65, no. 6, pp. 5213–5220, Jun. 2018.

[4].G.Carli and S. S. Williamson, "Technical considerations on power conversion for electric and plug-in hybrid electric vehicle battery charging in photovoltaic installations," *IEEE Transactions on Power Electronics*, vol. 28, no. 12, pp. 5784–5792, Dec. 2013.

[5]. V. D and V. John, "Dynamic modelling and analysis of buck converter based solar PV charge controller for improved MPPT performance," in *2018 IEEE International Conference on Power Electronics, Drives and Energy Systems (PEDES)*, pp. 1–6, Dec. 2018.

[6]. S. A. Singh, G. Carli, N. A. Azeez, and S. Williamson, "Modelling, design, control, and implementation of a modified z-source integrated PV/grid/EV dc charger/inverter," *IEEE Transactions on Industrial Electronics*, vol. 65, no. 6, pp. 5213–5220, Jun. 2018.

[7].G.Carli and S. S. Williamson, "Technical considerations on power conversion for electric and plug-in hybrid electric vehicle battery charging in photovoltaic installations," *IEEE Transactions on Power Electronics*, vol. 28, no. 12, pp. 5784–5792, Dec. 2013.